Simulating hydrodynamics in a Rushton turbine at different stirring velocities applied to non-Newtonian fluids

Simulating hydrodynamics in a Rushton turbine at different stirring velocities applied to non-Newtonian fluids

G Gelves[1]
[1] Universidad Francisco de Paula Santander, San José de Cúcuta, Colombia

E-mail: germanricardogz@ufps.edu.co

Abstract. In this work, gas-liquid hydrodynamics of a Rushton turbine was studied using Computational Fluid Dynamics. Different stirring conditions commonly used in fungal culture applications are simulated. Several scenarios are predicted related to gas-liquid mass transfer limitation. The above, reflected by low air dispersion reached and bubble size determinations caused by the non-Newtonian rheology, leading the process to obtain k_La values only in the order of 30 h^{-1} at high, stirring speeds. However, the high-power consumption in fungal culture in agitated tank bioreactors can be disadvantages in large-scale prototypes applied in non-Newtonian fluids. These Findings shown in this research should be considered as a primary criterion for optimizing mass transfer problems in large scale fungal culture applications.

1. Introduction

Performing required oxygen supply in aerobic cell cultures is still a common challenge in bioprocess engineering. In the case of filamentous culturing, mycelial growths are generally viscous and its non-Newtonian behavior influences transport and leads to reduced oxygen transfer [1]. Rushton turbine type impellers are extensively used in a large-scale application, but its potential implementation for mixing non-Newtonian fluids is doubtful based on its hydrodynamics disadvantages [1]. For this reason, knowing a detailed hydrodynamic behavior allows elucidating the basis for an improved mixing device. Computational fluid dynamics is a powerful software for simulating an aerobic process [2] due to its versatile codes for modelling multiphase applications. Even bubble breakup and coalescence from population balance models should be analyzed from computational fluid dynamics (CFD) since these phenomena lead to the formation of oxygen gradients and dissolved gases that can affect productivity in the aerobic process. The applicability of CFD is currently extended in areas of mixing equipment design, including from fluid rotation models in one phase [3-7], to the use of population balance models [8-25]. In addition to those mentioned, it is essential to highlight some cases of success in the design of devices using CFD, as reported by Gelves [26]. They designed a stirring-aeration system that managed to increase the transfer of oxygen 34 times higher than a conventional device in the culture of CHO cells for pharmaceutical applications. Later, Niño [27] proposed a device to improve mixing from CFD applied to the culture of animal cells in perfusion mode. Currently, the improvement of a stirring device is limited to empirical models that do not take into account hydrodynamics or transport phenomena that govern a bio-process. Based on the latter, these stages of the process are intuitive and experimental.

That is why the development of a prototype requires multiple steps, which is a disadvantage, due to the high costs and time of experimentation needed [28]. Based on the latter, one of the transcendental stages in agitation-aeration system design is to study the gas-liquid hydrodynamics widely used in the mixing of non-Newtonian solutions, which its effects on the bubble dispersion and mass transfer are still

poorly studied. For these reasons, this research is based on predicting possible mass transfer limitations using a conventional bioreactor (operated with Rushton Turbines) with applications in non-Newtonian fluids.

2. Computational fluid dynamics model and experiments

For modeling in CFD and experiments, a new Brunswick stirred tank bioreactor was used on a laboratory scale (10 litters of total volume) with 8 litters as working volume [29-33]. The tank that is characterized by the following dimensions: DT diameter: 0.21 m, height of the liquid (HL): 0.3 m, equipped with four baffles spaced at an angle of 90º with a width (Wb) of 0.1 DT, installed at a distance away from the walls of 0.010 m. The equipment has a six-blade Rushton turbine impeller with a diameter (Di) of 0.075 m. The air is supplied through a diffuser of 0.06 m in diameter. The operating conditions for simulations in CFD were defined based on typical parameters for fungal culture. The stirring ranges specified were 200 rpm, 400 rpm and 600 rpm and the aeration flow for all cases was adjusted to 1.0 vvm. To contemplate the viscosity achieved in a bioprocess, 0.25% xanthan gum was used. This allowed us to experimentally calculate the parameters of the viscosity model that were subsequently coupled to CFD. In this work, the Eulerian model was used and coupled to population balance models defined from Equation (1).

$$\frac{\partial}{\partial t}(\rho_G n_i) + \nabla \cdot \left(\rho_G \vec{U}_G n_i\right) = \rho_G \left(\Gamma_{B_{i_C}} - \Gamma_{D_{i_C}} + \Gamma_{B_{i_B}} - \Gamma_{D_{i_B}}\right). \quad (1)$$

Where n_i is the bubble numbers of classes i, $\Gamma_{B_{i_C}}$ and $\Gamma_{B_{i_B}}$ are the birth rates due to coalescence and breakage, respectively, $\Gamma_{D_{i_C}}$ and $\Gamma_{D_{i_B}}$ are the death rates. Previous research [34] has shown that fermentation of cultures with mycelium (highly viscous fluids) behave like a non-Newtonian fluid. Therefore, in this work, the power-law model was used to simulate the effects of viscosity μ_L as well as the algorithm of the discrete method [35-37] to solve the system of population balance equations for the bubbles. So that they are divided into different kinds of diameters as an input parameter. These equations are specified in [25,38,39]. Bubble breakup is modelled based on the interaction of the bubble's sizes v with the turbulent eddies ξ. The breakup rate is defined according to Equation (2) [4].

$$g(v')\beta(v|v') = k\int_{\xi_{min}}^{1} \frac{(1+\xi)^2}{\xi^{11/3}} \exp\left(-b\xi^{-11/3}\right) d\xi. \quad (2)$$

Coalescence between bubbles of size d_i and d_j is simulated considering the coalition of bubbles due to turbulence. Also, coalescence is usually defined as the product between collision frequency and coalescence efficiency, according to Coulaloglou and Tavlarides from Equation (3) [40].

$$a(v, v') = \frac{c_{c,1}\varepsilon^{1/3}\left(d_i+d_j\right)^2}{(1+\emptyset)}\left(d_i^{2/3} + d_j^{2/3}\right)^{1/2} \exp\left(-c_{c,2}\frac{\mu_L\rho_L\varepsilon}{\sigma^2(1+\emptyset)^3}\left(\frac{d_i d_j}{d_i+d_j}\right)^4\right). \quad (3)$$

Where ε is the dissipation turbulence energy, σ is the surface tension, and ρ_L is the liquid density. CFD model is verified considering the k_La values. Those latter were determined experimentally at a 10-liter scale, using 0.25% Xanthan gum to simulate the rheology effect of fungal culture.

For experimental determination of k_La, the bioreactor is gasified with air through the sparge and dissolved oxygen is monitored until saturation is reached. The dissolved oxygen concentration is measured using a sensor (InPro 6800, Mettler Toledo, Germany). Apparent viscosity is determined using a Brookfield DV-E viscometer applying cutting speeds in the range of 1 s^{-1} - 100 s^{-1}, to monitor the shear stress τ obtained at each rate. To determine the aerated power consumption P_g the Equation (4) [41,42] was used.

$$\frac{P_g}{P_{ug}} = C\left(\frac{V_S}{ND_i^3}\right)^{-0.38}\left(\frac{N^2D_i^3\rho}{\sigma}\right)^{-0.18}. \quad (4)$$

Where P_{ug} is the un-gassed power, C is a constant, V_S is the gas speed, N is the stirring speed, D_i is the impeller diameter, ρ is the liquid density and σ is the surface tension. The un gassed power is calculated from Equation (5).

$$P_{ug} = N_p\rho N_i^3 D_i^5. \quad (5)$$

Where N_p is the power number, the experimental data of k_La were adjusted according to the expression Xie [43] based on Equation (6), to obtain a model to perform the verifications of data collected from CFD.

$$k_La = C_1\left[\frac{P_g}{V}\right]^{0.45}[V_S]^{0.11}. \quad (6)$$

In which P_g is determined from the model proposed by Gill [41], C_1 is a model constant. For liquid phase mass transfer coefficient k_L determination from CFD, the Equation (7) was used and developed for bubbles in a turbulence field using the power-law model for this type of non-fluid Newtonians [44].

$$k_L = C_s\sqrt{D_L\left[\frac{\varepsilon\rho_i}{K}\right]^{\frac{1}{2[1+n]}}}. \quad (7)$$

Bubble interfacial area is calculated from Equation (8).

$$a = \frac{6\propto_G}{d_{32}}. \quad (8)$$

D_L is oxygen the diffusivity, K and n are rheological parameters, $\propto_G$ is the air volume fraction, d_{32} is the Sauter mean diameter. The k_La values obtained by CFD are calculated as the product between Equation (7) and Equation (8). The torque values M of the impellers were calculated by CFD, to determine the power consumed using the following mathematical expression based on Equation (9).

$$P_g = 2\pi N_i M. \quad (9)$$

3. Results

The main objective of this work was to analyze possible gas-liquid mass transfer in non-Newtonian fluids using a conventional Rushton turbine impeller. Air volume fraction, bubble sizes, velocity magnitude and k_La mass transfer coefficient were evaluated at different stirring conditions commonly used for fungal applications. The air volume fraction contours from the bioreactor operated at different agitation conditions (200 rpm - 600 rpm) are presented in Figure 1. It is shown that air distribution is only dispersed in areas closed to the turbine, while areas near the bioreactor wall are poorly oxygenated. The above, due to the strong resistance exerted by the viscosity in domains low stirred. The latter is because the shear rate is not sufficient to deform the fluid resistance. In such a way that heterogeneous environments and gradients could be generated and would the aerobic culture growth.

Based on mass transfer (detailed below), weak oxygenated zones are observed mainly at low stirring speeds (200 rpm). Even so, the increase in stirring speed (400 rpm and 600 rpm) fails to improve gas dispersion towards areas far from the impeller. This latter may indicate that limitations found are also associated with the geometry device. The above is supported by the characteristic hydrodynamics typical from a Rushton turbine [27], which is characterized by its ability to generate areas with varying degrees of mixing. These discrepancies can also be explained considering the velocity profiles. Figure 2 shows

the results of the velocity magnitude calculated from CFD at different operating conditions. It is observed highest velocity magnitude occurs in areas closed to the turbine at 200 rpm, while dead zones are shown far away from the stirring zone. This behavior can lead to the formation of air bubble ducts or "caverns" (a common term used in non-Newtonian fluids to describe the air accumulation) due to poor dispersion.

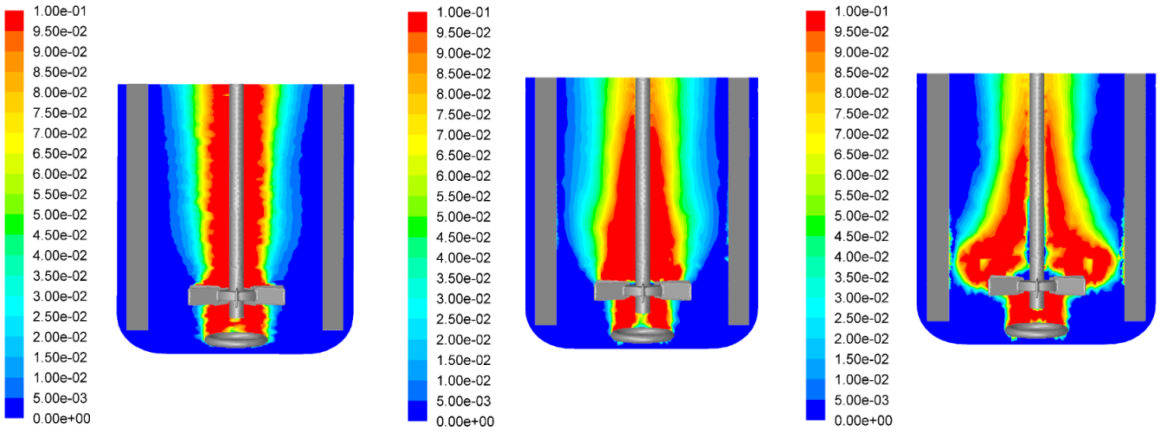

Figure 1. Air volume fraction contours. (a) N_i: 200 rpm, (b) N_i: 400 rpm, and (c) N_i: 600 rpm.

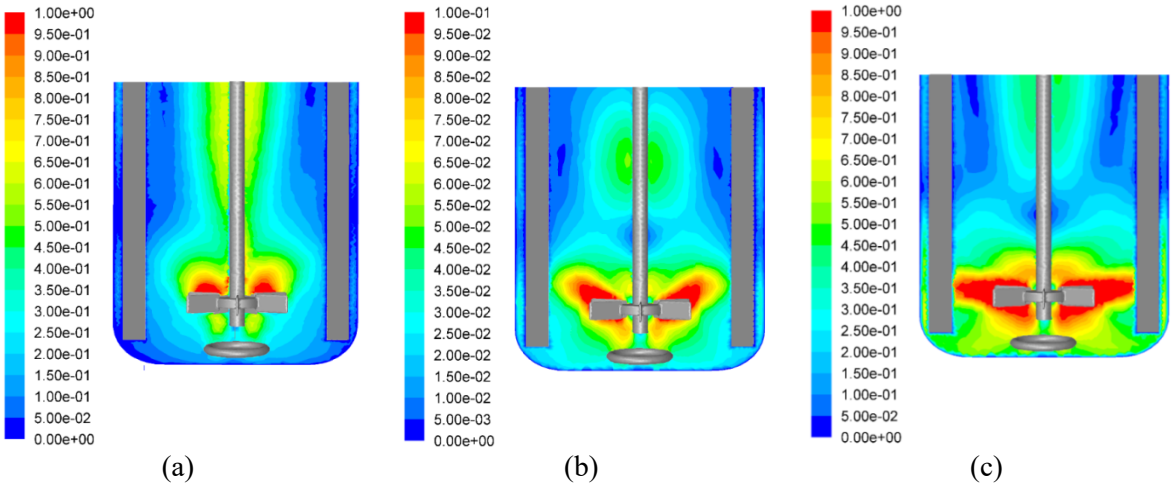

Figure 2. Velocity magnitude contours v/v_{tip} (-). (a) N_i: 200 rpm, (b) N_i: 400 rpm and (c) N_i: 600 rpm.

These limitations found significantly affect the bubble sizes in a bioreactor. That is why it is necessary to determine an integral parameter that allows the prediction of an average bubble diameter as a result of breakup and coalescence. Thus, population balance models have been coupled to hydrodynamics and the rheological model used in this work to calculate the Sauter mean diameter. The latter is an integral parameter that allows the phenomena impacts of mass transfer mentioned here. Figure 3 shows Sauter mean diameter simulated for a 10-liter bioreactor (Rushton turbine) operated at different stirring conditions.

It is evident the high degree of coalescence that can be seen in all cases (Figure 3). The large-sized bubbles in the order of 5 mm - 10 mm negatively influences the bubble dispersion so that air remains less time in the bioreactor and the bubble breakup is weak. The latter generates stagnant areas at the bottom of the bioreactor, as shown in Figure 4, and air bubbles do not reach to be dispersed. Therefore, these areas of poor mixing tend to be dominated by the high resistance exerted by viscosity towards mass transfer due to insufficient values of shear velocity in these stagnant areas. This phenomenon can

be seen significantly at low, stirring speeds (200 rpm; see Figure 4), so that the turbine's rotation speed does not generate sufficient velocity profiles to cause breakage, bringing the process to a bubble coalescence state. When the stirring velocity is increased, better radial velocity profiles are generated to counteract the effects of air buoyancy. In this way, the breakup phenomenon takes special consideration, indicating that radial velocity is an essential factor for a device optimization focuses on increasing mass transfer in non-Newtonian fluids since smaller bubbles are generated.

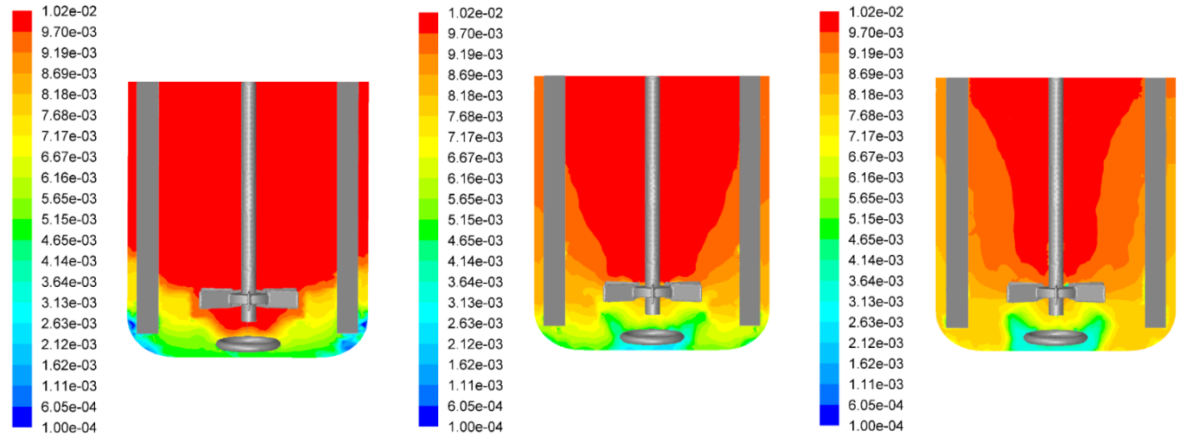

Figure 3. Sauter mean diameter contours (m). (a) N_i: 200 rpm, (b) N_i: 400 rpm, and (c) N_i: 600 rpm.

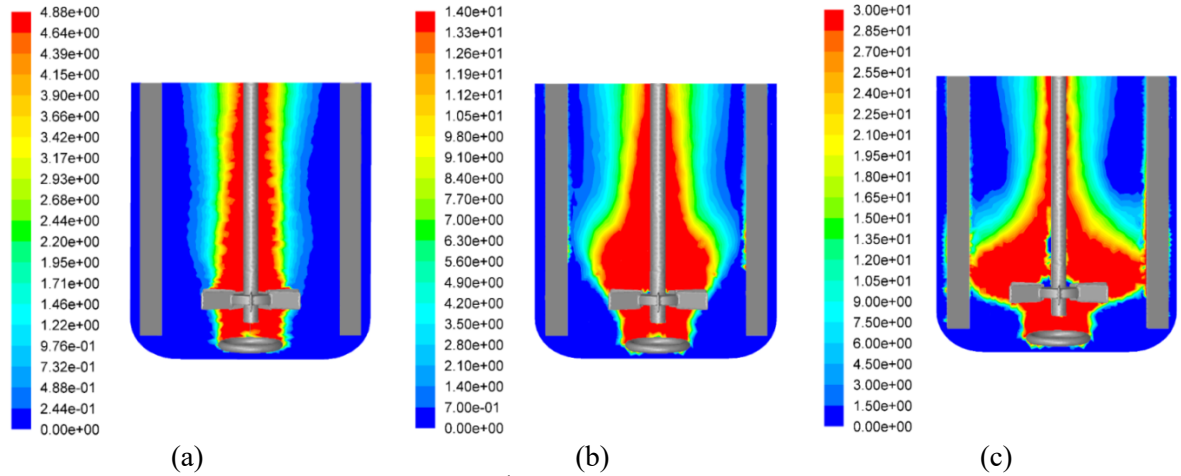

Figure 4. Mass transfer coefficient $k_L a$ (h^{-1}). (a) N_i: 200 rpm, (b) N_i: 400 rpm, and (c) N_i: 600 rpm.

In a non-Newtonian fluid, the apparent viscosity is the primary resistance to the gas-liquid mass transfer since this limits the fluid layer deformation. So that the rheological parameters strongly influence the k_La values. The oxygen transfer rate can control the overall velocity of an aerobic biological process and as a consequence, it can determine the bioreactor capacity. For this reason, k_La has been widely used as an operating criterion in many aerobic processes [45]. k_La values were calculated from CFD using the Higbies penetration theory. The k_La value is obtained from the information calculated from the liquid phase mass transfer coefficient k_L and the interfacial bubble area a [46]. The results of CFD simulations of the oxygen transfer coefficient are presented in Figure 4. Based on this information, similarities are observed between the values calculated by CFD and the data obtained experimentally (Table 1). The latter means that the breakup and coalescence models predict with a proper approach to the mass transfer phenomena involved in the criteria studied.

Table 1. k_La values calculated from experimental data (Exp.) and CFD simulations.

N_i (rpm)	200		400		600	
k_La (h^{-1})	Exp.	CFD	Exp.	CFD	Exp.	CFD
Value	5.4	4.88	13.68	14.00	30.60	30.00

The power consumption required by a mechanical stirrer is an essential parameter in the design of impeller devices applied to non-Newtonian fluids. In this study, the power consumption obtained by CFD was determined from Equation (9) by calculating the torque M (described previously). Additional to the above for verifying breakage and coalescence model impacts on the non-Newtonian fluid, an Equation (6) was used to calculate the gassed power consumption [41]. This, to compare the power data obtained by CFD and those determined by the expression above. In Figure 5, similarities are observed in the results obtained by CFD and the expression calculated for the power with aeration, which indicates that the formulation of the mathematical model obtained in this investigation shows an acceptable precision.

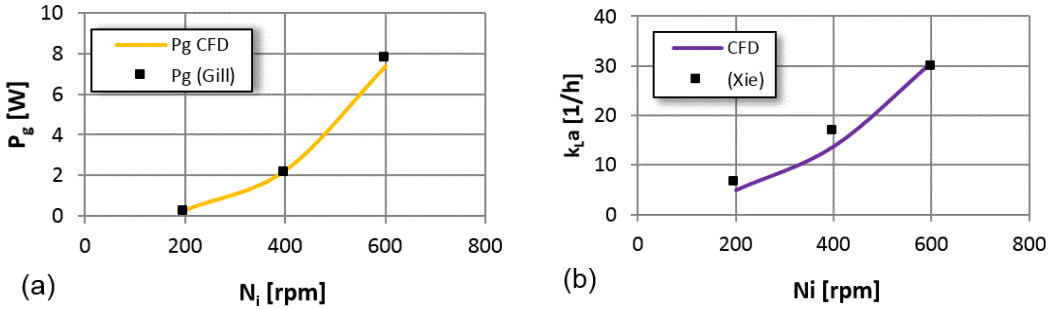

Figure 5. (a) Gassed power impeller P_g (W) calculated from CFD and correlation (Gill). (b) k_La values (h^{-1}) calculated from CFD and expression (Xie).

Figure 5 also shows the k_La data by CFD and compared it with the expression of Xie [119], which was used as a reference point to verify the simulations with CFD. Acceptable accuracy is observed concerning the experimental data obtained in this investigation. The results demonstrate the proportional effect of power impeller required to increase k_La in each case. This event has already been verified by experimental research [47-49]. The challenges aimed to improve mass transfer in non-Newtonian fluids should be addressed to the dispersion of uniform bubbles to all bioreactor areas, as well as generation of flow patterns allowing to reduce the stagnant low mass transfer areas. According to the above, it is evident that the device designed also counteracts the effects of resistance to movement, which are induced by the viscosity of the non-Newtonian fluid studied (Xanthan Gum).

4. Conclusions

The CFD model used in this research simulates the most important effects that influence the k_La values in non-Newtonian fluids and have been satisfactorily verified concerning experimental data. Using CFD, mass transfer limitations were found associated with the geometry of the impeller device (Rushton Turbine). The above, explained by the low air dispersion and large bubble sizes. The Sauter mean diameter and flow patterns are some of the limiting variables to be taken into account in the design of a stirring-aeration device.

References

[1] Niño L, Gelves R, Ali H, Solsvik J, Jakobsen H 2019 *Chemical Engineering Science* **211** 1
[2] Gelves R, Benavides A, Quintero J 2013 *Ingeniare Revista Chilena de Ingeniería* **21** 347
[3] Jenne M, Reuss M 1999 *Chemical Engineering Science* **54(17)** 3921

[4] Luo J, Issaand R, Gosman A 1994 *Chemical Engineering Symposium Series. Institution of Chemical Engineers* **136** 549
[5] Micale G, Brucato, A Grisafi F 1999 *American Institute of Chemical Engineering* **45(3)** 445
[6] Rutherford K, Lee, Mahmoudi K, Yianneskis M 1996 *American Institute of Chemical Engineering* **42** 332
[7] Tabor A, Gosman G, Issa R 1996 *American Institute of Chemical Engineering Symposium Series* **140** 25
[8] Solsvik J, Jakobsen H 2016 *American Institute of Chemical Engineering* **62(5)** 1795
[9] Kerdouss F, Bannari A, Proulx P, Bannari R, Skrga M, Labrecque Y 2012 *Computers and Chemical Engineering* **32** 1943
[10] Kerdouss F, Kiss L, Proulx P, Bilodeauand, Dupuis C 2005 *International Journal of Chemical Reactor Engineering* **3** 35
[11] Kerdouss F, Bannari A, Proulx P, Bannari R, Skrgaand M, Labrecque Y 2007 *Computers and Chemical Engineering* **3** 1
[12] Lane L, Schwarz M, Evans M 2005 *Chemical Engineering Science* **60** 2203
[13] Venneker C, Derksen H 2002 *American Institute of Chemical Engineering* **48(4)** 673
[14] Scargiali F, D'Orazio A, Grisafi F, Brucato 2007 *Chemical Engineering Research and Design* **85(5)** 637
[15] Kasat G, Pandit A B, Ranade V V 2008 *International Journal of Chemical Reactor Engineering* **6** 1
[16] Nino L, Peñuela M, Gelves G 2018 *International Journal of Applied Engineering Research* **13(11)** 9353
[17] Ranade V V, Dommeti J B 1990 *Chemical Engineering Communications* **74(4)** 476
[18] Jakobsen H, Lindborg H, Dorao C 2005 *Industrial Engineering of Chemical Research* **44(14)** 5107
[19] Jahoda M, Tomášková L, Moštěk M 2009 *Chemical Engineering Research and Design* **87(4)** 460
[20] Luo H, Svendsen H 1996 *American Institute of Chemical Engineering* **42(5)** 1225
[21] Laakkonen M, Moilanen P, Alopaeus A, Aittamaa J 2007 *Chemical Engineering Research and Design* **85(5)** 665
[22] Panneerselvam R, Savithri S 2011 *Chemical Engineering Science* **66(14)** 14
[23] Martinov M, Vlaev S 2002 *Chemical and Biochemical Engineering* **16(1)** 1
[24] Tiefeng W, Jinfu W 2007 *Chemical Engineering Science* **62(24)** 7107
[25] Chen P, Sanyal J, Dudukovic M P 2005 *Chemical Engineering Science* **60(4)** 1085
[26] Gelves R, Dietrich A, Takors R 2014 *Bioprocess and Biosystems Engineering* **37** 365
[27] Niño L, Peñuela M, Gelves G 2016 *International Journal of Applied Engineering Research* **11(9)** 6097
[28] Raikar B, Bhatia R, Malone F, Henson A 2009 *Chemical Engineering Science* **64** 2433
[29] Niño L, Gelves G 2015 *Revista Facultad de Ingeniería Universidad de Antioquia* **75** 163
[30] Junker A 2004 *Journal of Bioscience and Bioengineering* **97(6)** 347
[31] Alopaeus V, Koskinen K 1999 *Chemical Engineering Science* **54(24)** 5887
[32] Ishii M, Zuber N 1979 *American Institute of Chemical Engineering* **25(5)** 843
[33] Elgobashiand S E, Rizk M A 1989 *International Journal of Multiphase Fl*ow **15(1)** 119
[34] Chavez-Parga M, Gonzalez-Ortega O, Negrete-Rodriguez M, Medina-Torres L, Silva E 2007 *World Journal of Microbiology and Biotechnology* **23(5)** 615
[35] Hounslow M, Ryall R, Marschall V 1988 *American Institute of Chemical Engineering* **34(11)** 1821
[36] Litster D, Smit D, Hounslow M 1995 *American Institute of Chemical Engineering* **41(3)** 591
[37] Niño L, Peñuela M, Gelves G 2018 *Indian Journal of Science and Technology* **11** 1
[38] Hagesaether L, Jakobsen H A, Hjarbo K, Svendsen H F 2000 A coalescence and breakup module for implementation in CFD codes *European Symposium on Computer-Aided Process Engineering* ed Pierucci S (Netherlands: Elsevier Science) p 367
[39] Sanyal J, Marchisio D L, Fox R O, Dhanasekharan K 2005 *Industrial Engineering and Chemical Research* **44(14)** 5063
[40] Coulaloglou C, Tavlarides L 1977 *Chemical Engineering Science* **32** 1289
[41] Gil N, Appleton M, Baganz F, Lye G 2008 *Biotechnology and Bioengineering* **100(6)** 1144
[42] Luong H T, Volesky B 1979 *American Institute of Chemical Engineering* **25(5)** 893
[43] Xie M 2014 *Chemical Engineering Science* **106** 144
[44] Valverde M R, Bettega B, Badino A C 2016 *Theoretical Foundations in Chemical Engineering* **50(6)** 945
[45] Ochoa F, Gomez E 2009 *Biotechnology Advances* **27** 153
[46] Dhanasekharan K, Sanyal J, Jain J, Haidari A 2005 *Chemical Engineering Science* **60** 213
[47] Flórez F, Torre M 1997 *Journal of Fermentation and Bioengineering* **6** 561
[48] Arjunwadkar S J, Sarvanan K, Kulkarni P, Pandit A B 1998 *Biochemical Engineering Journal* **2** 99
[49] Shukla V K, Parasu U, Kulkarni P R, Pandit A B 2001 *Biochemical Engineering Journal* **8** 19